Assembling coordination networks of bis-amido pyridines *via* hydrogen bonds: isostructurality and large hydrophobic cavities for guest inclusion†‡

Lalit Rajput and Kumar Biradha*

Received (in Montpellier, France) 27th January 2010, Accepted 7th April 2010
DOI: 10.1039/c0nj00070a

The reactions of bis(3-pyridylcarboxamido)alkanes (amides, **1**) and bis(3-pyridyl)alkanediamides (reverse amides, **2**) with $Cu(SCN)_2$ in the presence of various guests afforded 22 crystalline complexes containing 1D and 2D coordination networks with or without guest inclusion. In these complexes, the ratio of metal to ligand is either 1 : 1 or 1 : 2, despite carrying out all the reactions by taking metal and ligand in 1 : 2 ratio. The recognition of coordination networks *via* amide-to-amide hydrogen bonds in the form of β-sheet was observed in the complexes containing metal to ligand ratio (1 : 2). Various guest molecules such as DMF, nitrobenzene, benzonitrile, 1,4-dihalobenzenes, phenanthrene, biphenyl, anthracene, 9-anthraldehyde and pyrene were found to include in these networks depending on the lengths of the spacers in **1** or **2**. The ligands **1** or **2** with shorter spacers such as $-(CH_2)_2-$ and $-(CH_2)_4-$ have shown no consistency or preference to any particular network geometry. However the ligands with longer spacers such as $-(CH_2)_6-$, $-(CH_2)_8-$ or phenyl have exhibited consistency in network geometries. The iso-structurality between the coordination polymers of amides and reverse amides was observed for ligands with longer spacers such as $-(CH_2)_6-$ and $-(C_6H_4)-$. The spacer $-(CH_2)_n-$ found to exhibit different conformations for accommodating the guests of different sizes and shapes. The guest occupied volume in these crystal lattices varies from 27% to 60%.

Introduction

The gigantic rise in the literature of coordination polymers (CPs) owes to their fascinating architectures, intriguing topologies and their functional properties.[1,2] Several rigid and flexible ligands were designed and employed for the construction of CPs.[3,4] The prediction of the topologies of CPs containing rigid ligand is more precise compared to those containing a flexible ligand. The adaptability of various conformations and coordination modes by flexible ligands diversifies the network topologies and complicates the prediction of structural properties. In addition to the nature of the ligand, the network topologies were shown to depend on several other factors such as metal–ligand ratios, counter anions, metal coordination geometries, pH values, guest molecules and the process of crystallization.[5] All these factors make coordination polymers modular in nature to offer great variety of functional materials for a given set of components. Due to the dependence of CPs geometry on various factors as mentioned above, a systematic investigation is required to understand the importance of each factor. The key strategy for this exercise is to vary one of those factors while keeping the other factors constant. Here, we have carried out such a systematic investigation to explore the ligand effect by gradually varying the lengths of the ligand in the form of number of $-(CH_2)-$ groups while keeping the metal ion and anion constant (Scheme 1).

Recently, we have initiated studies on transfer of molecular recognition information from organic materials to their organic–inorganic materials (CPs) by using bis-amido pyridine derivatives (**1** and **2**). Ideally these ligands have two functional groups: pyridine to coordinate with the metal and amide for recognition of CPs *via* N–H···O hydrogen bonds. We have already explored the crystal structures of both the analogues (**1** and **2**) and found that although these two have the same combination of functional groups at the molecular level, behave very differently at supramolecular level. In case of **1**, the presence of pyridine groups does not interfere in the formation of amide-to-amide hydrogen bonds whereas in case of **2**, pyridine groups exhibit interference and disrupts the amide-to-amide recognition pattern. The phenyl-substituted analogues of **1** and **2** or pyridine substituted analogues of **1**

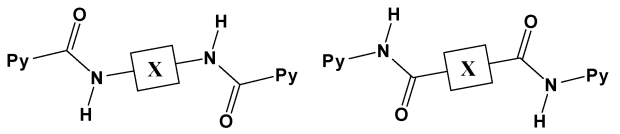

1a; $-(CH_2)_2-$, 3-Py **1b**; $-(CH_2)_4-$, 3-Py **1c**; $-(CH_2)_6-$, 3-Py **1d**; $-(CH_2)_8-$, 3-Py **1e**; $-(C_6H_4)-$, 3-Py
2a; $-(CH_2)_2-$, 3-Py **2b**; $-(CH_2)_4-$, 3-Py **2c**; $-(CH_2)_6-$, 3-Py **2d**; $-(CH_2)_8-$, 3-Py **2e**; $-(C_6H_4)-$, 3-Py

Scheme 1 Exo bidentate ligands bis(pyridylcarboxamido)alkanes (amides, **1**) and bis(pyridyl)alkanediamides (reverse amides, **2**).

Department of Chemistry, Indian Institute of Technology, Kharagpur-721302, India. E-mail: kbiradha@chem.iitkgp.ernet.in; Fax: +91-3222-282252; Tel: +91-3222-283346

† This article is part of a themed issue on Coordination polymers: structure and function.

‡ Electronic supplementary information (ESI) available: IR, TGA and crystallographic information of complexes. CCDC reference numbers 763762–763774. For ESI and crystallographic data in CIF or other electronic format see DOI: 10.1039/c0nj00070a

have exhibited two types of N–H···O hydrogen bond patterns: (1) β-sheet; (2) 2D-layer.[6]

We have also shown that the analogues of **1** and **2** are capable of forming various CPs (open 2D-networks, chiral 2D-networks, interpenetrated 2D-networks (both parallel and perpendicular mode) and 3D pseudo diamondoid ($6^5$8-topology) networks) with Cu(II) salts of ClO_4^-, NO_3^-, SCN^- and PF_6^-.[7] In several instances these coordination networks shown to recognize each other through amide-to-amide hydrogen bonds namely β-sheet hydrogen bonding pattern (Scheme 2). In parallel with our studies several other groups demonstrated on CPs of the ligands containing urea as spacer. In these CPs, urea often found to interact with the anions or with the solvent of crystallization rather than with itself.[8] Further, the CPs with ligands containing mono-amide as spacer have also been shown to form functional porous materials.[9]

Here we present our results of reactions of **1** and **2** with $Cu(SCN)_2$ in the presence of various guest molecules. We have recently communicated that the coordination networks of **1** and **2** with Cu(II) are iso-structural when the spacers are $-(CH_2)_6-$ or $-C_6H_4-$ and anion is SCN.[7g] The inclusion of bigger guest molecules such as phenanthrene, pyrene, 1,4-di-iodobenzene and 1,4-di-bromobenzene was also observed in these isostructural CPs. These results prompted us for an extensive investigation of CPs of the analogues of **1** and **2** with $Cu(SCN)_2$. Our studies on the reactions of **1** and **2** with $Cu(SCN)_2$ resulted in the crystals of 22 complexes of CPs which will be analyzed in terms of their networks, hydrogen bonding patterns and guest inclusion. In this paper we address the following aspects:

(1) Isostructurality of CPs of **1** and **2**

(2) Assembling of coordination networks *via* amide-to-amide recognition

(3) Effect of various conformations on the network geometries

(4) Role of guest molecules in templation of the network geometries

(5) Role of solvent used for complexation reaction

(6) Guest exchange by dissolving the complex in the presence of new guest

Results & discussion

The reactions are performed in three ways. The first one deals with the addition of DMF solution of **1** or **2** with guest or without to the methanolic solution of $Cu(NO_3)_2$ and NaSCN (**3–9** & **12–17**). The second one involves guest exchange method by dissolving the complex of one guest in the DMF solution of a new guest molecule (**10** & **11**). The complexes **18** and **19** were prepared by layering methanolic solution of $Cu(NO_3)_2$ and NaSCN over the DMF-benzonitrile/nitrobenzene and EtOH–$CHCl_3$ solution of the ligand respectively. We have obtained the crystals of total of 22 complexes using analogues of **1** and **2**. In these complexes eight corresponds to ligand **1** while fourteen corresponds to ligand **2**. Although the results obtained here indicate that the metal to ligand ratios vary from 1 : 1 (**3–13**) to 1 : 2 (**14–19**), we note here that all these

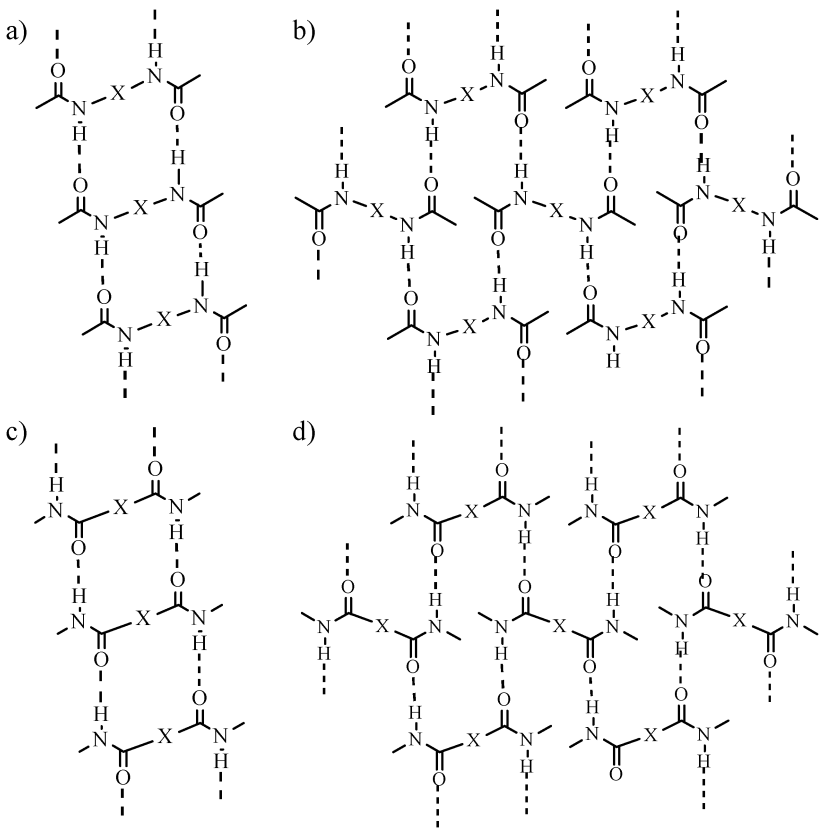

Scheme 2 Hydrogen bonding patterns: (a) β-sheet and (b) 2D-layers in amides and (c) β-sheet and (d) 2D layer in reverse amides.

reactions were performed by taking the metal to ligand ratio of 1 : 2.

The crystal structures of complexes **3–19** were determined and analyzed in terms of coordination network geometries, recognition of networks through hydrogen bonds, and guest inclusion. The crystal structures of complexes of **14**, **15**, **17**, **18a** and **19** were reported by us previously.[7] The pertinent crystallographic details, bond lengths around Cu(II), and geometrical parameters of hydrogen bonds involving amides were given in Table 1–4. The Cu(II) and the ligands sit on inversion center in the complexes **3–7**, **9–11**, **13**, **16** and **18b** while in **12** only the Cu(II) atoms lie on inversion center. In the following sections we discuss our results by categorizing these complexes based on metal to ligand ratios, network topologies and guest inclusion.

{Cu(**2a**)$(SCN)_2(DMF)_2$}$_n$, **3**	{[Cu(**2a**)$(SCN)_2$]·2(DMF)·nitrobenzene}$_n$, **12**
{[Cu(**2a**)$(SCN)_2(DMF)_2$]·2(DMF)}$_n$, **4**	{[Cu(**1b**)$(SCN)_2$]·2(nitrobenzene)}$_n$, **13**
{Cu(**2b**)$(SCN)_2(DMF)_2$}$_n$, **5**	{[Cu(**1c**)$_2(SCN)_2$]·2(Guest)}$_n$, **14**
{[Cu(**1c**)$(SCN)_2(H_2O)_2$]·2(H_2O)}$_n$, **6**	{[Cu(**2c**)$_2(SCN)_2$]·2(Guest)}$_n$, **15**
{[Cu(**1d**)$(SCN)_2(DMF)_2$]·2(H2O}$_n$, **7**	{[Cu(**2d**)$_2(SCN)_2$]·2(9-anthraldehyde)}$_n$, **16**
{[Cu(**1e**)$(SCN)_2(DMF)_2$]·2(DMF)}$_n$, **8**	{[Cu(**1a**)$_2(SCN)_2$]·6(nitrobenzene)}$_n$, **17**
{[Cu(**2d**)$(SCN)_2(DMF)_2$]·anthracene}$_n$, **9**	{[Cu(**2e**)$_2(SCN)_2$]·2(Guest)}$_n$, **18**
{[Cu(**2d**)$(SCN)_2(DMF)_2$]·biphenyl}$_n$, **10**	{Cu(**1e**)$_2(SCN)_2$}$_n$, **19**
{[Cu(**2d**)$(SCN)_2(DMF)_2$]·pyrene}$_n$, **11**	

Guest: 1,4-dibromobenzene (**14a**, **15b**); pheneanthrene (**14b**, **15d**); 1,4-diiodobenzene (**15a**); pyrene (**15c**); benzonitrile (**18a**); nitrobenzene (**18b**).

One-dimensional chains with metal to ligand ratio of 1 : 1 (3–8)

The reaction of **2a** with $Cu(SCN)_2$ resulted in the crystals of two complexes **3** and **4** in the same reaction flask. The crystal structures of **3** and **4** reveal that both contain 1D chain with same coordination environment around Cu(II) but exhibit certain interesting differences (Fig. 1). The separation of metal atoms is shorter in **3** (14.689 Å) compared to that of **4** (16.517 Å). This difference can be attributed to the non-planarity of **2a** in **3** due to the C–C–N–C(O) torsion of 50° instead of usual *anti* geometry with the torsion of 180°. In addition, the crystal lattice of **4** contains the DMF guest molecule. In **3**, 1D-chains lead to the formation of a 2D-layer *via* N–H···S hydrogen bonds between amide N–H and SCN anion (synthon-**I**). The amide carbonyl joins these layers *via* bifurcated C–H···O hydrogen bonds with pyridine C–H groups. In complex **4**, the N–H groups are hydrogen bonded to solvent DMF molecules. Therefore the crystal packing is governed by weak hydrogen bonds such as C–H···O between carbonyl group and pyridine C–H groups. Guest DMF occupies 32% volume of the crystal lattice and stays in between the two-dimensional layers.

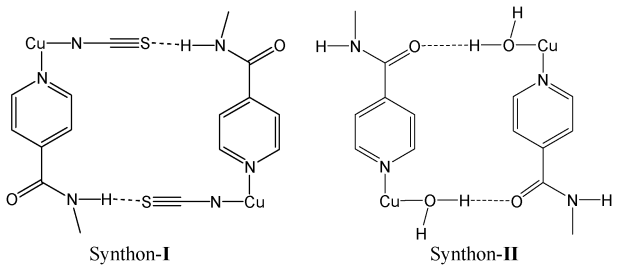

The next higher analogue **2b** forms complex **5**, the crystal structure of **5** is somewhat similar to that of complex **3**. The ligand **2b** does not exhibit planarity, similar to **2a** in **3**, due to the *gauche-anti-gauche* conformation of butyl chain (Fig. 2a). The ligands join the metal atoms with a distance of 15.146 Å which is in between those of **3** and **4**. Similar to **3**, the 1D-chains are joined into two-dimensional layer *via* N–H···S hydrogen bonds (synthon-**I**) (Fig. 2b). Carbonyl groups of amides join the layers *via* O-bifurcated C–H···O hydrogen bonds (Fig. 2c). From the TGA analysis it is observed that the complex looses the coordinated DMF molecules at 170 °C and from 170 °C onwards ligand degradation takes place.

The complexation of the ligand **1c** with Cu(II) in DMF–MeOH resulted in the crystals of complexes **6** and **14**. The crystal structure of **14** will be discussed under the complexes containing 1 : 2 metal-to-ligand ratio. In the crystal structure of **6**, unlike the above complexes, water molecules coordinate at axial positions of Cu(II) but not DMF (Fig. 3a). The ligand **1c** does not exhibit linearity and adopts the *gauche-anti-anti-anti-gauche* conformation as a result it separates the metal atoms by 16.57 Å. Amide N–H groups are hydrogen bonded to free water molecules, while amide carbonyls of adjacent chains are joined together by coordinated water molecules *via* synthon-**II** to form a two-dimensional layer (Fig. 3b). These layers are joined together through short S···S contacts (3.364 Å) between SCN ions which is a unique feature of this complex while in other cases S-atoms are involved in N–H···S or O–H···S hydrogen bonds (Fig. 3c). From the TGA analysis it is observed that the complex **6** loses free and coordinated waters molecules together at 147 °C.

It is important to note here that the crystals of complex **7** were obtained only in the presence of phenanthrene. In **7**, the ligand **1d** is not linear as the octyl spacer exhibits *gauche-anti-anti-anti-anti-anti-gauche* conformation (Fig. 4a) and the metal atoms are linked by the longest distance of 19.834 Å. This structure better be explained in terms of hydrogen bonding as there exists some significant hydrogen bonding interactions. In this structure the ligands themselves self assemble into two-dimensional layer *via* amide-to-amide N–H···O hydrogen bonds (Fig. 4b and c). This pattern is one of the two patterns (β-sheet & 2D-layer) exhibited by the ligands of **1** or **2** containing ethyl or butyl spacers in their own crystal structures.[6] However, longer spacers such as $-(CH_2)_6-$ and $-(CH_2)_8-$ have exhibited only β-sheet which has been transferred into their CPs. Therefore this is the first example of a 2D-layer pattern for octyl spacer of **1** and also first example of CP containing such N–H···O hydrogen bonding pattern. Further, the $Cu(SCN)_2$ ions self-assemble *via* O–H···S interaction with free water molecules (Fig. 4d). These two layers are

Table 1 Crystallographic parameters for complexes **3–13**, **16** and **18b**

Compound	**3**	**4**	**5**	**6**	**7**	**8**	**9**
Formula	$C_{19}H_{21}N_7O_3S_2Cu_1$	$C_{28}H_{42}N_{10}O_6S_2Cu_1$	$C_{24}H_{32}N_8O_4S_2Cu_1$	$C_{20}H_{30}N_6O_6S_2Cu_1$	$C_{28}H_{44}N_8O_6S_2Cu_1$	$C_{32}H_{42}N_{10}O_6S_2Cu_1$	$C_{42}H_{50}N_8O_4S_2Cu_1$
M. Wt.	523.09	742.38	624.24	574.13	716.37	790.42	858.56
T/K	293(2)	293(2)	293(2)	293(2)	293(2)	293(2)	293(2)
System	Triclinic	Triclinic	Triclinic	Triclinic	Monoclinic	Triclinic	Triclinic
Space group	$P\bar{1}$	$P\bar{1}$	$P\bar{1}$	$P\bar{1}$	$P2_1/c$	$P\bar{1}$	$P\bar{1}$
a/Å	7.3067(6)	8.899(4)	7.474(3)	7.808(3)	13.243(3)	10.069(3)	7.4123(4)
b/Å	8.9226(8)	9.728(4)	9.371(3)	8.946(3)	14.680(3)	14.339(3)	10.5479(6)
c/Å	9.7407(8)	12.736(6)	10.441(4)	10.837(6)	9.166(2)	14.469(4)	14.0519(8)
α (°)	76.265(2)	77.685(1)	80.42(1)	102.02(1)	90	75.382(7)	83.276 (2)
β (°)	88.597(2)	71.18(1)	89.87(1)	104.36(2)	109.618(6)	85.836(7)	75.937(2)
γ (°)	70.435(2)	68.75(1)	76.38(1)	111.25(1)	90	76.313(7)	89.908(2)
Vol. (Å^3)	580.21(9)	966.8(7)	700.3(4)	645.2(5)	1678.5(6)	1963.8(8)	1058.0(1)
Z	1	1	1	1	2	2	1
D_c/Mg m^{-3}	1.497	1.275	1.480	1.478	1.374	1.337	1.348
R_1 ($I > 2\sigma(I)$)	0.0624	0.0707	0.0353	0.0424	0.0612	0.0583	0.0458
wR_2 (on F^2, all data)	0.1934	0.2363	0.1035	0.1286	0.1656	0.1866	0.1401

Compound	**10**	**11**	**12**	**13**	**16**	**18b**
Formula	$C_{40}H_{50}N_8O_4S_2Cu_1$	$C_{44}H_{50}N_8O_4S_2Cu_1$	$C_{28}H_{33}N_9O_6S_2Cu_1$	$C_{30}H_{28}N_8O_6S_2Cu_1$	$C_{72}H_{72}N_{10}O_6S_2Cu_1$	$C_{50}H_{38}N_{12}O_8S_2Cu_1$
M. Wt.	834.54	882.58	719.29	724.26	1301.06	1062.58
T/K	293(2)	293(2)	293(2)	293(2)	293(2)	293(2)
System	Triclinic	Triclinic	Triclinic	Triclinic	Monoclinic	Triclinic
Space Group	$P\bar{1}$	$P\bar{1}$	$P\bar{1}$	$P\bar{1}$	$P2_1/n$	$P\bar{1}$
a/Å	7.4307(3)	7.430(1)	11.099(3)	7.312(2)	9.845(1)	8.1263(1)
b/Å	10.5364(4)	10.703(2)	12.396(3)	9.953(2)	14.921(2)	10.0055(2)
c/Å	14.0517(5)	14.433(3)	13.677(3)	12.917(3)	22.721(3)	15.295(3)
α (°)	91.139(1)	105.255(5)	95.279(7)	99.909(6)	90	73.118(4)
β (°)	103.470(1)	100.958(6)	98.762(7)	105.708(6)	97.076(4)	87.475(4)
γ (°)	91.626(1)	90.074(5)	111.365(7)	110.183(6)	90	87.115(4)
Vol. (Å^3)	1069.06(7)	1085.4(4)	1709.5(7)	811.9(3)	3312.2(7)	1187.9(3)
Z	1	1	2	1	2	1
D_c (Mg m^{-3})	1.296	1.350	1.397	1.481	1.305	1.485
R_1 ($I > 2\sigma(I)$)	0.0418	0.0738	0.0860	0.0324	0.0478	0.0381
wR_2 (on F^2, all data)	0.1307	0.2044	0.2407	0.0960	0.1356	0.1056

Table 2 Bond lengths around Cu(II) center and interpanar angle (θ) between amide and pyridine planes in the crystals structures of complexes **3–19**

Complex	Cu–N (Ligand)	Cu–N (SCN)	Cu–O/S	Interplanar angle θ/°
3	2.035(5)	1.941(7)	2.272(1)[a]	9.60
4	2.038(4)	1.970(4)	2.473(5)[a]	11.51
5	2.032(2)	1.971(2)	2.533(2)[a]	5.96
6	2.039(3)	1.945(3)	2.587(4)[b]	3.19
7	2.050(4)	1.955(5)	2.465(6)[a]	25.30
8	2.029(3)	1.959(4)	2.504(4)[a]	22.61, 26.57
	2.043(3)	1.966(4)	2.505(4)[a]	
9	2.031(2)	1.973(3)	2.487(3)[a]	6.80
10	2.034(2)	1.966(3)	2.477(3)[a]	4.68
11	2.031(4)	1.968(5)	2.509(4)[a]	9.62
12	2.047(4)	1.939(6)	2.980(2)[c]	6.34, 7.80
	2.041(5)	1.953(5)	2.980(2)[c]	
13	2.0212(2)	1.9635(2)	2.5513(2)[d]	37.18
14a	2.059(4), 2.542(4)	1.959(4)	—	1.59, 45.09
14b	2.056(3), 2.570(3)	1.941(3)	—	8.14, 51.81
15a	2.078(6), 2.498(7)	1.985(7)	—	16.66, 49.78
15b	2.069(5), 2.495(5)	1.954(6)	—	14.14, 49.06
15c	2.080(2), 2.500(2)	1.964(2)	—	9.61, 46.28
15d	2.074(2), 2.526(8)	1.955(2)	—	9.60, 46.28
16	2.076(2), 2.484(2)	1.955(2)	—	4.70, 52.46
17	2.048(5), 2.642(5)	1.953(5)	—	6.60, 40.34
18a	2.067(2), 2.619(2)	1.968(2)	—	27.63, 44.18
18b	2.098(1), 2.531(2)	1.9683(2)	—	27.00, 43.33
19	2.060(4), 2.494(4)	1.965(4)	—	22.92, 26.73

[a] DMF "O". [b] H_2O "O". [c] SCN "O". [d] Amide "O" coordination.

Table 3 Geometrical parameters of hydrogen bonds in the crystal structures of complexes **3–13**, **16** and **18b**

Complex	Type	H···A/Å	D···A/Å	D–H···A (°)
3	N(21)–H(21)···S(100)[a]	2.61	3.461(6)	168
	C(14)–H(14)···O(21)[b]	2.69	3.27(1)	121
4	N(22)–H(22)···O(200)	1.98	2.838(7)	180
	C(25)–H(25)···O(11)[c]	2.58	3.267(6)	131
5	N(12)–H(12)···S(200)[d]	2.63	3.484(3)	171
	C(14)–H(14)···O(16)[e]	2.61	3.262(3)	128
6	N(11)–H(11)···O(1W)[f]	2.09	2.897(5)	157
	C(22)–H(22)···O(1W)	2.47	3.373(5)	163
7	N(21)–H(21)···O(16)[g]	2.13	2.939(6)	157
8	N(31)–H(31)···O(500)[h]	2.01	2.816(5)	155
	N(32)–H(32)···O(600)[i]	2.11	2.942(6)	162
	C(22)–H(22)···O(400)[j]	2.55	3.164(5)	124
	C(24)–H(24)···O(16)[k]	2.42	3.246(5)	148
9	N(12)–H(12)···S(200)[l]	2.69	3.531(2)	168
	C(14)–H(14)···O(21)[m]	2.55	3.192(4)	127
10	N(21)–H(21)···S(200)[n]	2.63	3.490(2)	174
	C(14)–H(14)···O(11)[o]	2.46	3.133(4)	130
11	N(21)–H(21)···S(100)[p]	2.68	3.534(5)	174
	C(14)–H(14)···O(20)[q]	2.54	3.188(7)	128
12	N(12)–H(12)···O(400)[r]	1.94	2.80(1)	176
	N(22)–H(22)···O(300)[s]	2.01	2.85(1)	163
13	N(20)–H(20)···O(1A)[t]	2.42	2.959(3)	121
	C(13)–H(13)···O(2A)[u]	2.50	3.223(4)	135
16	C(15)–H(15)···O(1A)[v]	2.34	3.263(4)	174
18b	C(15B)–H(15B)···O(21A)[w]	2.40	3.215(3)	145

Symmetry operators: [a] $2-x,-y,1-z$. [b] $-1+x,y,z$. [c] $2-x,-y,1-z$. [d] $-x,1-y,1-z$. [e] $1+x,y,z$. [f] $1-x,-y,1-z$. [g] $x,-1/2-y,1/2+z$. [h] $2-x,2-y,1-z$. [i] $2-x,3-y,2-z$. [j] $1+x,y,1+z$. [k] $2-x,3-y,2-z$. [l] $x,1+y,z$. [m] $-1+x,y,z$. [n] $x,-1+y,z$. [o] $-1+x,y,z$. [p] $3-x,-y,-z$. [q] $-1+x,y,z$. [r] $x,1+y,z$. [s] $1-x,1-y,1-z$. [t] $1-x,-y,1-z$. [u] $1+x,y,z$. [v] $x,-1+y,-1+z$. [w] $x,-1+y,z$.

Table 4 Geometrical parameters of amide-to-amide hydrogen bonds in the form of β-sheet in the crystal structures of complexes **14–19**

	Intra network		Inter network	
Complex	N···O/Å	N–H···O (°)	N···O/Å	N–H···O (°)
14a	3.022(6)[a]	163	2.969(6)[b]	169
14b	3.000(4)[c]	164	2.953(4)[d]	163
15a	2.950(9)[e]	159	2.939(9)[f]	156
15b	2.936(7)[g]	162	2.899(7)[h]	156
15c	3.153(3)[i]	163	2.884(3)[j]	146
15d	3.056(3)[k]	169	2.848(3)[l]	147
16	2.925(3)[m]	171	2.859(3)[n]	167
17	2.989(7)[o]	164	—	—
	2.933(7)	157		
18a	2.911(3)	156	—	—
	3.063(3)[p]	143		
18b	2.921(2)	156	—	—
	3.085(2)[q]	141		
19	2.924(5)[r]	150	—	—
	3.154(5)	152		

Symmetry operators: [a] $3-x,2-y,1-z$. [b] $3-x,2-y,1-z$. [c] $1-x,-y,1-z$. [d] $1-x,-y,1-z$. [e] $2-x,1-y,1-z$. [f] $2-x,2-y,1-z$. [g] $-1-x,-1-y,-z$. [h] $-1-x,-2-y,-z$. [i] $1-x,-y,-1-z$. [j] $2-x,-y,-1-z$. [k] $1-x,-y,-1-z$. [l] $1+x,y,z$. [m] $-x,-y,-1-z$. [n] $1-x,-y,-1-z$. [o] $-1+x,y,z$. [p] $x,1+y,z$. [q] $x,-1+y,z$. [r] $1+x,-1+y,z$. The CCDC numbers for the structures published in ref. 7*d* and *g*: (**14a**) 720555, (**14b**) 720556, (**15a**) 720551, (**15b**) 720552, (**15c**) 720553, (**15d**) 720554, (**17**) 286845, (**18a**) 720557, (**19**) 286846.

joined into three dimensional architecture *via* coordination of pyridine and Cu(II).

The ligand **1e** found to form two complexes (**8** and **19**) with $Cu(SCN)_2$ depending on the reaction conditions. When the molecule **1e** is complexed with $Cu(SCN)_2$ by direct mixing in DMF–MeOH produced the crystal of complex **8**. The complex **19** will be discussed under the complexes containing metal-to-ligand ratio of 1 : 2. The composition of complex **8** is similar to that of complex **4** and has two free DMF molecules as guest apart from two coordinated DMF molecules. The free DMF is hydrogen bonded to amide -NH of **1e** (Fig. 5a) and the ligand **1e** links the metal atoms with a distance of 18.218 Å. The joining of the chains occurs through weak C–H···O hydrogen bonds, between pyridine C–H groups and amide carbonyl, and weak C–H···N hydrogen bonds between C–H of coordinated DMF and amide N-atom (Fig. 5b and c). Thiocyanates engage in weak C–H···S hydrogen bond with pyridine and guest DMF C–H groups. DMF occupies 29% volume of the crystal lattice.

One-dimensional chains with M to L ratio of 1 : 1 and guest inclusion (9–11)

The reactions of **2d** with $Cu(SCN)_2$, in the absence of guest molecules failed to produce crystalline products while the presence of anthracene resulted in the crystals of **9**. Our efforts for inclusion of some other guest molecules by following the similar procedure were not successful to give suitable crystalline materials for single crystal diffraction study. However, by dissolving crystals of **9** in DMF solution of biphenyl or pyrene resulted in the crystals of **10** and **11** respectively. The crystal structure analysis of **9–11** reveals that all contain similar one-dimensional chain with some minor differences in the geometry of alkyl chain (Fig. 6a–c). Interestingly, the alkyl chain found to adopt its conformation

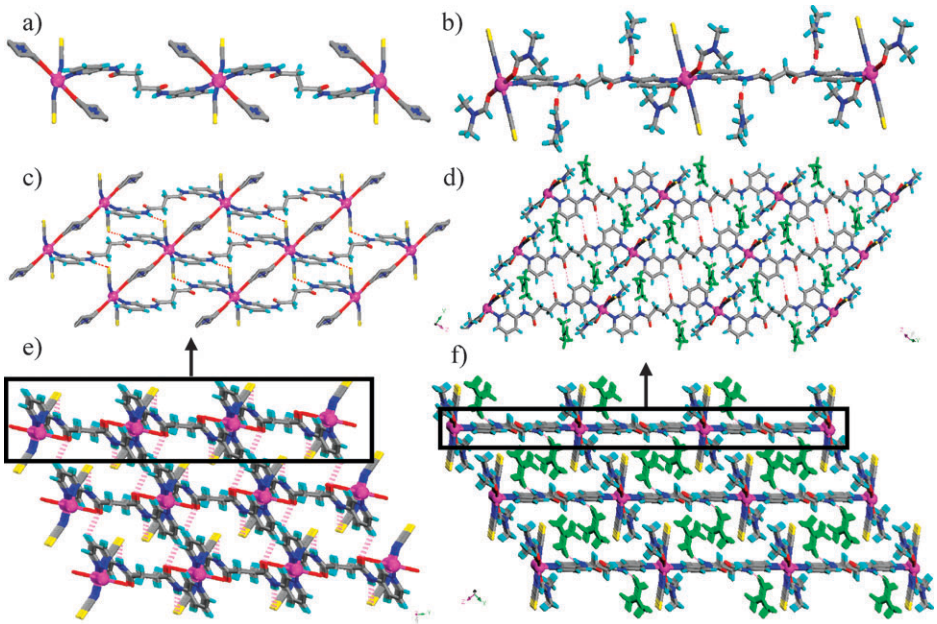

Fig. 1 Illustrations for the crystal structures of **3** and **4**: one-dimensional chains in (a) **3**, DMF molecules are disordered and (b) **4**, free DMF molecules are hydrogen bonded to the amides; packing of 1D-chains into 2D-layers in (c) **3** *via* N–H···S hydrogen bond (synthon-**I**) and in (d) **4** *via* C–H···O hydrogen bonds; packing of 2D-layers *via* (e) C–H···O hydrogen bonds in **3** and (f) C–H···π interactions in **4**.

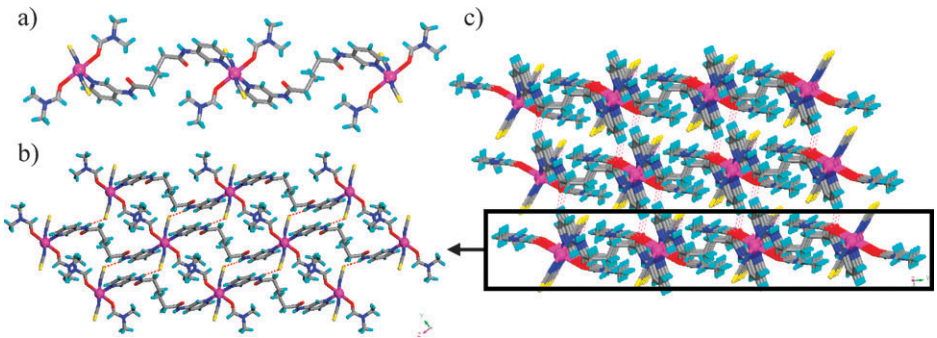

Fig. 2 Illustrations for the crystal structure of **5**: (a) 1D chain, (b) packing of 1D-chains *via* N–H···S hydrogen bond (synthon-**I**) and (c) 3D packing of the layers *via* C–H···O hydrogen bond.

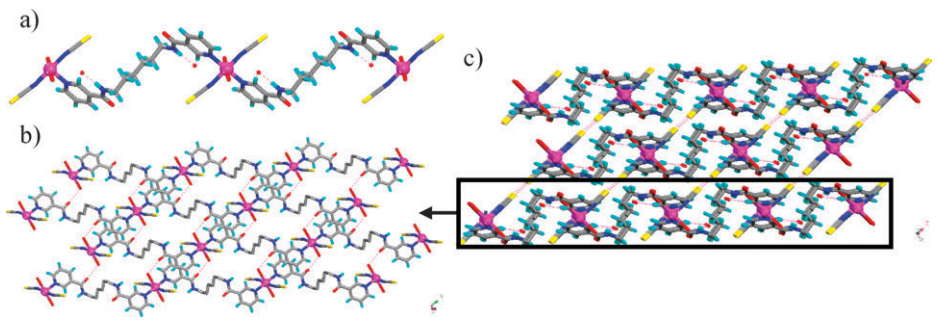

Fig. 3 Illustrations for the crystal structure of **6**: (a) 1D-chain, (b) layer of the chains *via* O–H···O hydrogen bonds (synthon-**II**) and (c) packing of the layers through S···S interactions.

or length according to the demands of the size of guest molecule. The ligand exhibits *gauche-anti-gauche-anti-gauche-anti-gauche* conformation in **9** to accommodate relatively smaller guest anthracene. While it exhibits *gauche-anti-anti-anti-anti-gauche* conformation in **10** to accommodate medium size guest such as biphenyl. In **11**, the bigger guest such as pyrene is accommodated as the ligand exhibits all *anti* conformations. Accordingly the metal-to-metal separation in one-dimensional chains also differs: 18.532 Å, 17.395 Å and 20.464 Å in **9**, **10** and **11** respectively. In all the three complexes

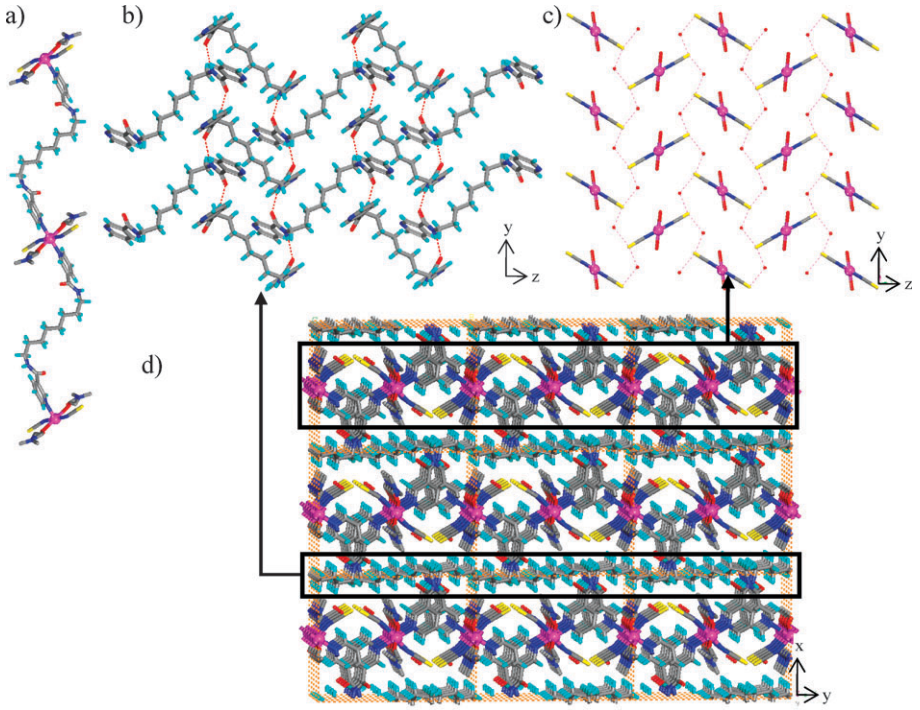

Fig. 4 Illustrations for the crystal structure of complex **7**: (a) 1D-chain (b) 2D-layer of **1d** *via* amide-to-amide hydrogen bonds (*bc*-plane); (c) assembling of $Cu(H_2O)_2(SCN)_2$ units into 2D-layer by water molecules with the help of O–H···S hydrogen bonds (*bc*-plane); (d) assembling of 2D-layers into a 3D-architecture *via* coordination bonds (*ab*-plane).

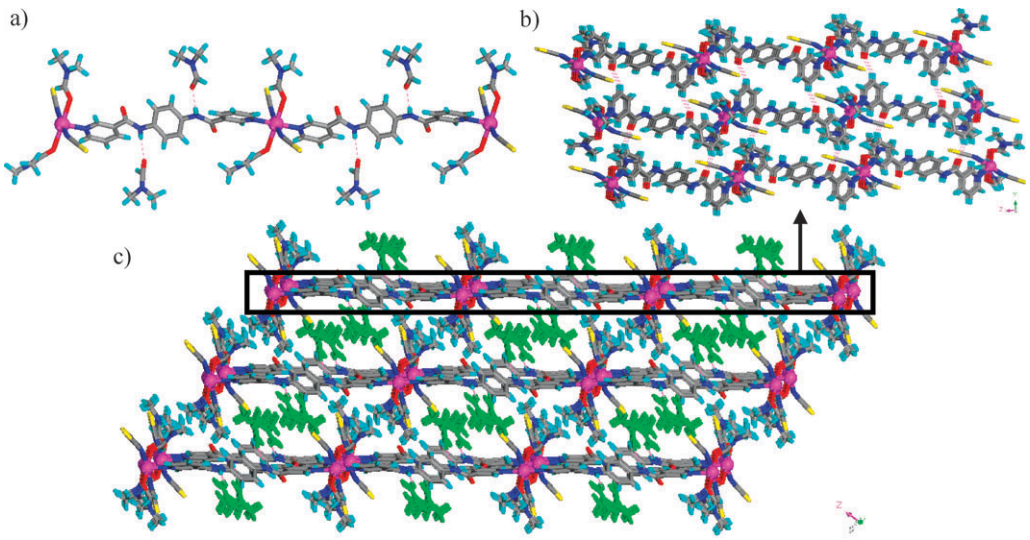

Fig. 5 Illustrations for the crystal structure of complex **8**: (a) 1D-chain; (b) joining of 1D-chains *via* C–H···O hydrogen bonds into a 2D-layer; and (c) packing of the layers *via* weak hydrophobic interactions between free DMF molecules (free DMF molecules are shown in green color).

the 1D-chains are joined *via* N–H···S hydrogen bonds (synthon-**I**) into a two-dimensional layer containing cavities for guest inclusion (Fig. 6d). These layers pack on each other *via* C–H···O hydrogen bonds between carbonyl and pyridine C–H groups such that continuous channels are formed. These channels are occupied by the column of coordinated DMF and guest molecules (Fig. 6e). In other words, the guest molecules are locked in the cavities by the coordinated DMF molecules. In **9**, both the methyl groups of DMF molecules are close to each other with C···C distances of 3.99 Å and 4.17 Å. Whereas in **10** only one methyl group from each DMF participates in close contact 3.88 Å. Interestingly, no such methyl···methyl contacts were observed in **11**. The methyl groups are also involved in C–H···π interactions with guest molecules: C···π-plane distances 3.50–3.78 Å in **9**, 3.62–3.77 Å in **10** and 3.50–3.75 Å in **11**. The guest occupied volumes in **9**, **10** and **11** are 27%, 28% and 30% of the crystal volumes respectively.

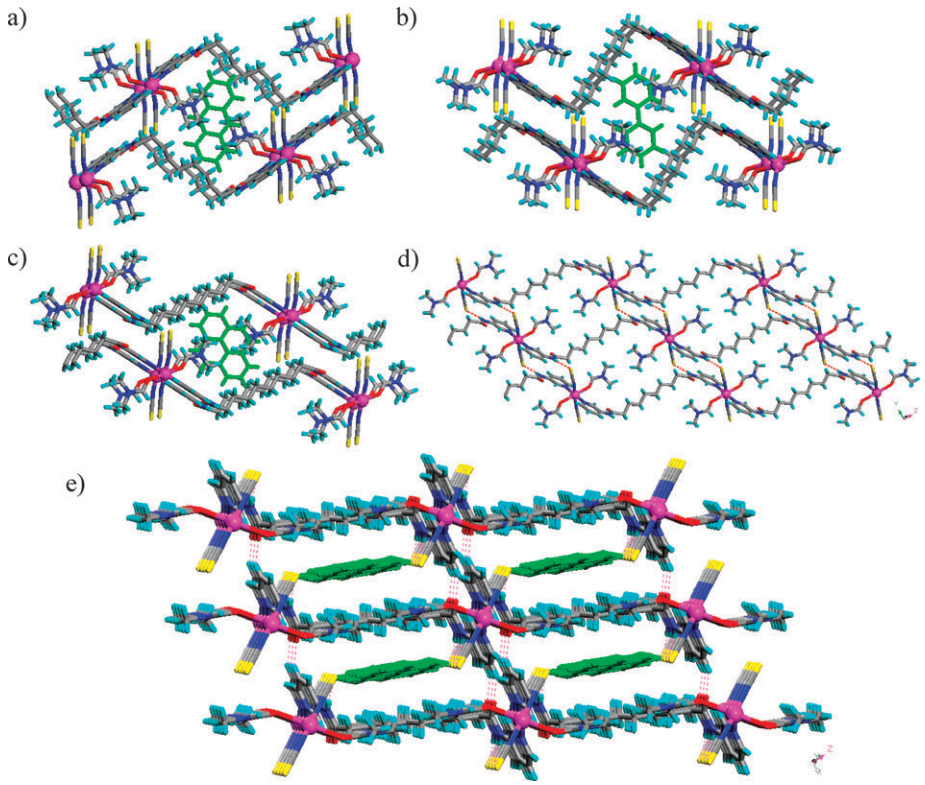

Fig. 6 Illustrations for the crystal structure of complexes **9–11**. The inclusion of guests (a) anthracene in **9**, (b) biphenyl in **10** and (c) pyrene in **11** (notice the change in conformations of the octyl spacer of the ligand); (d) assembling of 1D-chains *via* N–H···S hydrogen bond (synthon-**I**) in **11**; (e) packing of the layers *via* C–H···O hydrogen bonds and inclusion of guest molecules between the layers.

Two dimensional layers with M to L ratio of 1 : 1 and guest inclusion (12–13)

The reaction of **2a** and **1b** with $Cu(SCN)_2$ in the presence of nitrobenzene resulted in the crystals of **12** and **13** respectively. In both the complexes the Cu(II) center has octahedral coordination, the equatorial sites are occupied by two pyridine units of the ligand and two N-atoms of SCN while the axial sites are not occupied by solvents such as H_2O or DMF which is the common feature observed in all the complexes discussed above. The axial sites in **12** are occupied by the S-atom of SCN *via* bridging, while in **13** the amide carbonyls occupy the axial sites. This type of bridging generates two-dimensional networks in both cases. The network in **12** contains cavities of dimension 16.91 Å × 17.59 Å and these cavities are filled by nitrobenzene molecules (Fig. 7a). Amide –NH is involved in N–H···O hydrogen bond with guest DMF molecules which are occupied between the layers (Fig. 7b). These 2D layers have interlayer separation of 9.445 Å and interact with each other *via* C–H···O hydrogen bonds between amide carbonyl and pyridine. DMF and nitrobenzene occupies 53% of volume in the crystal lattice.

Whereas the 2D-layers in **13** do not contain any cavities, however the guest nitrobenzene molecules are included between the layers (Fig. 8). The nitro group of nitrobenzene hydrogen bonds to the adjacent layers *via* N–H···O with amide -NH and C–H···O with pyridine –CH group. Two molecules of nitrobenzene guest are observed per formula unit of the complex. Amide –NH also participates (H bifurcation) in N–H···S hydrogen bond within the 2D layer. The guest occupied volume is 43% with the inter layer separation of 11.886 Å. The amide coordination of the ligand **1b** observed here is unique and unusual in this series of thiocyanate complexes. The TGA analysis suggests that the complex looses both the nitrobenzene molecules at 185 °C and from 185 °C onwards ligand degradation takes place.

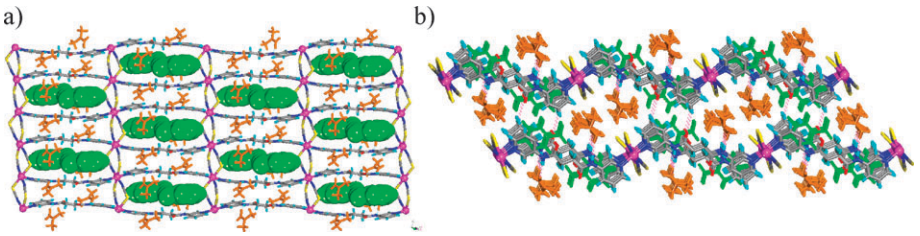

Fig. 7 Illustrations for the crystal structure of complex **12**: (a) 2D-network *via* thiocyanate bridging of Cu(**2a**) chains (nitrobenzene is shown in space fill mode); (b) side view of the packing of the layers.

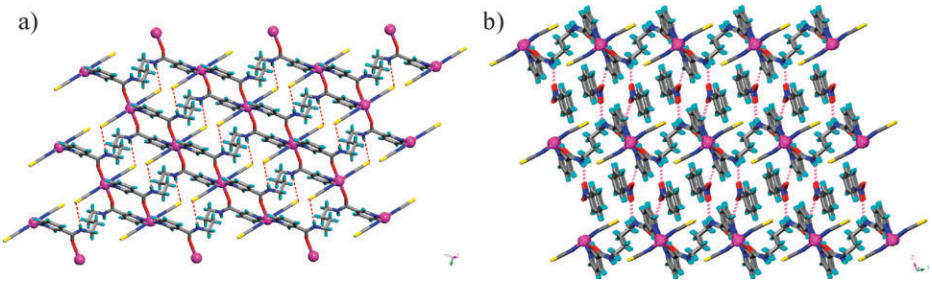

Fig. 8 Illustrations for the crystal structure of complex **13**: (a) linking of Cu(**1b**) chains into 2D-network *via* amide carbonyl coordination (notice intra-layer N–H···S hydrogen bonds); (b) inclusion of nitrobenzene between the layers.

One-dimensional chains with M to L ratio of 1 : 2 and guest inclusion (14–16)

All the complexes discussed above do not contain amide-to-amide hydrogen bonds except in one case (**7**). The coordinated solvent molecules or SCN ions interrupt the self aggregation of ligands *via* N–H···O hydrogen bonds. Notably the above complexes contain both amides and reverse amides with all possible five spacers. However, our reactions of Cu(II) with both amides and reverse amides containing longer spacers in the presence of certain guest molecules resulted in the association of networks *via* anticipated amide-to-amide hydrogen bonds.

The complexation of **1c** with $Cu(SCN)_2$ in the presence of 1,4-dibromobenzene or pheneanthrene resulted in the complexes of **14a** or **14b** respectively. While the same reaction with **2c** also resulted in the similar type of complexes but exhibited in the inclusion of four types of guest molecules 1,4-diiodobenzene (**15a**), 1,4-dibromobenzene (**15b**), pyrene (**15c**) and phenanthrene (**15d**).

The crystal structure of all these complexes contains one-dimensional networks with metal-to-ligand ratio of 1 : 2. In all the six cases, the Cu(II) centers have octahedral coordination with two pyridyl ligands and two SCN anions in the equatorial plane while the remaining two pyridyl groups in axial position. All exhibit 1D-coordination networks which contain intra and inter network β-sheet hydrogen bonding between the ligands (Fig. 9a and b).

The 2D-layers pack in two different modes depending on the nature of the guest molecules present. In case of 1,4-dihalobenzene as guests, the layers exhibit perfect flatness. In the packing, adjacent layers are related by translation symmetry and overlapped on each other with an interlayer separation of ~8.0–8.3 Å. The guest molecules form columns *via* C–H···I or C–H···Br interactions and exist between the layers. The halogen atoms which are involved in C–H···halogen interactions also engage in halogen bond with SCN anion. While in case of pyrene or phenanthrene as guest molecules, the layers are corrugated and packed in a slipped fashion. Interestingly, the adjacent layers are related by a screw axis and are separated by ~7.5 Å. The guest molecules are sandwiched by the pyridine moiety of one layer and amide moiety of the adjacent layers and are occupied in channels which exist along the diagonals of the layer. The edges of the guest molecules interact with each other *via* C–H···π interactions (Fig. 9c and d).

The guest molecules occupy 34%, 42%, 35%, 33%, 42% and 40% of the crystal volumes of **14a**, **14b**, **15a**, **15b**, **15c** and **15d** respectively. It is interesting to note that both the packing patterns observed in these structures have almost similar packing index of ~68%. The crystal structures reveal complete isostructrality between coordination networks of amides and reverse amides.

However the longer spacer such as $-(CH_2)_8-$ exhibited guest selectivity in the formation of above described networks. It was found that the ligand **2d** in the presence of 9-anthraldehyde can template the networks similar to the ones observed in **14** or **15** (Fig. 10a). The reaction of **2d** with $Cu(SCN)_2$ in the presence of 9-anthraldehyde resulted in the crystals of **16**.

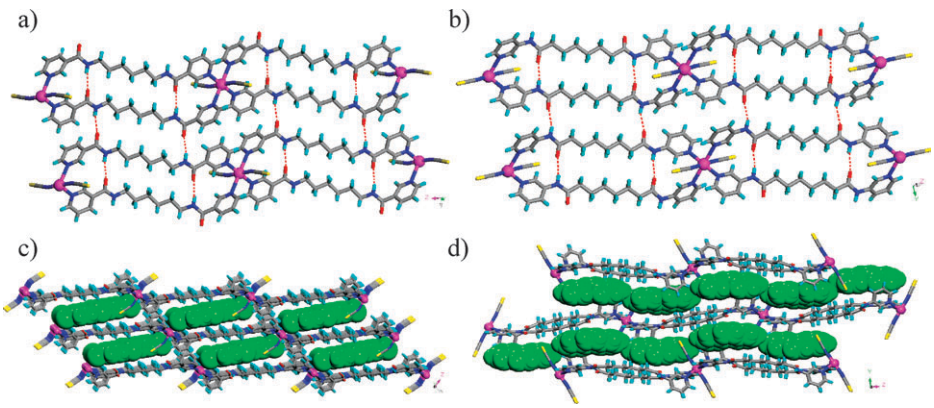

Fig. 9 β-Sheet hydrogen bonding observed in the complexes (a) **14** and (b) **15**. Packing of the two dimensional layers with the inclusion of guest (c) 1,4-di-iodobenzene and (d) phenanthrene (notice the differences in packing, guest molecules were shown in green color).

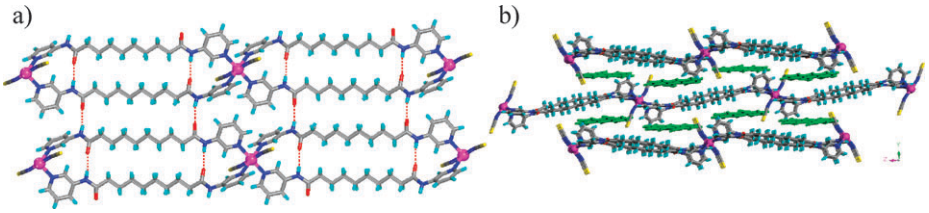

Fig. 10 Illustrations for the crystal structure of complex **16**: (a) *β*-sheet hydrogen bonding and (b) inclusion of 9-anthraldehyde between the layers. (Guest molecules shown in green.)

The crystal structure of **16** reveals the presence of 1D chain which is isostructural with the chains observed in complexes **14** and **15**. These chains also exhibit intra and inter network *β*-sheet hydrogen bonding to form a similar two-dimensional layers. The layers are corrugated and packed in a slipped fashion as observed in complexes **14b**, **15c** and **15d** with pyrene or phenanthrene guest (Fig. 10b). Guest molecules are sandwiched by the pyridine moiety from one layer and amide moiety of the adjacent layer forming column of 9-anthraldehyde molecules along the diagonals of the layer. The aldehyde carbonyl is interacting with pyridine –CH *via* C–H···O (2.336 Å, 173.60°, 3.262 Å) hydrogen bond whereas the phenyl rings are engaged in C–H···π interactions (closest C···C distance: 3.662 Å) with the alkyl spacers and pyridine (C···C distance 3.853 Å). The guest molecules in the column are not interacting with each other and they contribute 42% to the crystal volume. The interlayer separation observed is 7.461 Å. The TGA analysis suggests that the complex **16** loses both the 9-anthraldehyde molecules at 279 °C. Here it is interesting to note that the presence of other guest molecules such as anthracene, biphenyl and pyrene templated different one-dimensional chains (**9**, **10** & **11**) with metal-to-ligand ratios of 1 : 1. Similar reactions with **1d** failed to produce the crystals of inclusion complex.

Two-dimensional layers with 1 : 2 M to L ratio and with or without guest inclusion (17–19)

The reactions of **1a** with $Cu(SCN)_2$ in the presence of nitrobenzene produced the crystals of **17**. The crystals of **17** can be obtained either by layering procedure in MeOH–nitrobenzne solvents or by direct mixing of $Cu(SCN)_2$ and **1a** in DMF, MeOH and nitrobenzene. The crystal structure of **17** exhibits a two-dimensional layer (Fig. 11a). The Cu(II) has a highly distorted octahedral geometry with four units of **1a** at equatorial positions and two SCN anions at axial positions. The two-dimensional layer has a (4,4)-geometry with rhomboidal cavities. In the layer the ligands have intra network *β*-sheet hydrogen bonds. The interlayer separation of the coordination layers is as high as 11 Å as one layer of nitrobenzene molecules occupies the space between the layers (Fig. 11b). The layer of nitrobenzene composed of hexameric aggregates of nitrobenzene molecules (Fig. 11c) which interact with each other *via* six C–H···O hydrogen bonds. The guest molecule aggregation seems to be an important factor in obtaining the two-dimensional layer as the use of other guest molecules such as benzene, xylene, toluene, naphthalene and benzoic acid in place of nitrobenzene failed to give proper crystalline materials.

The repeat of the similar reaction with ligands **2e** or **1e** resulted in the single crystals of complexes **18** and **19** respectively. The crystal structures exhibit similar two-dimensional layer as above (Fig. 12a and 13a). However, these two structures differ with respect to the guest inclusion. The complex **18** has benzonitrile (**18a**) or nitrobenzene (**18b**) as guest while the complex **19** does not have any guest molecule (Fig. 12b and 13b). In both the structures, the (4,4)-networks contain intra layer *β*-sheet hydrogen bonds between the ligands as well as aromatic edge-to-face interactions between

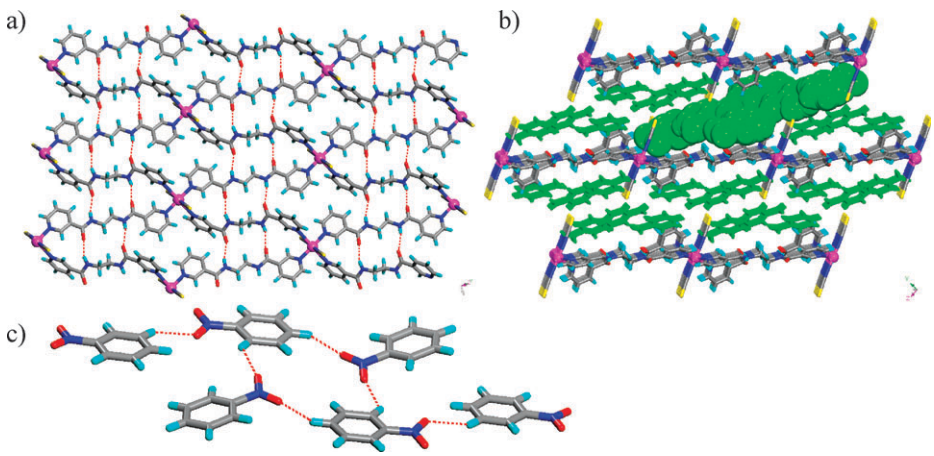

Fig. 11 Illustrations for the crystal structure of complex **17**: (a) (4,4)-layer containing intralayer *β*-sheet hydrogen bonds; (b) entrapment of layer of nitrobenzene between the (4,4)-coordination layers; (c) C–H···O hydrogen bonded hexameric aggregate of nitrobenzene molecules in the layer (shown in spacefill mode in 10b).

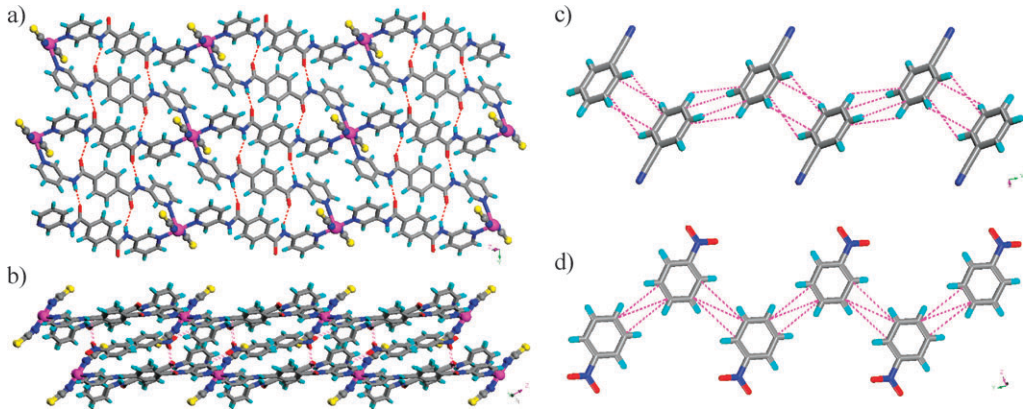

Fig. 12 Illustrations for the crystal structure of complex **18**: (a) Intralayer β-sheet hydrogen bonds in the crystal structure of **18a**, compare the layers with those in Fig. 8 and 9; (b) side view of β-sheet network in **18b**. Interactions between the guest molecules (c) benzonitrile in **18a** and (d) nitrobenzene in **18b**.

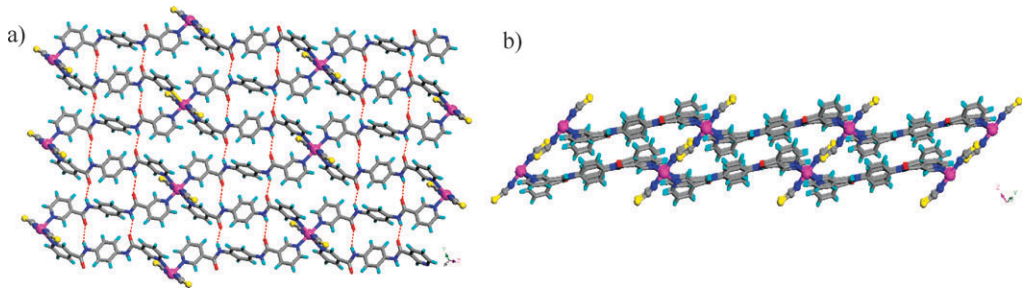

Fig. 13 Intralayer β-sheet hydrogen bonds in the crystal structure of (a) **18** and b) **19**, compare the layers with those in Fig. 8 and 9. Side view of β-sheet network (c) in **18a**, (d) **18b** and (e) **19**. Interactions between the guest molecules (f) benzonitrile in **18a** and (g) nitrobenzene in **18b**.

the phenyl spacers and also between the pyridyl groups. In **19**, these layers stack on each other with an interlayer separation of 5.224 Å suggesting strong aromatic edge-to-face interactions between the layers. While in complex **18**, the packing of the layers creates channels between the layers which are filled by the column of guest molecules. In the columns, the guest molecules interact with each other *via* edge-to-edge aromatic interactions between C_6H_5 units while the cyano (**18a**) and nitro (**18b**) groups interact with walls of the channels *via* C–H···O and C–H···N interactions respectively (Fig. 12c and d). The S-atom of the thicyanate is engaged in C–H···S hydrogen bond with the central phenyl ring of **2e** in the complexes **18a** and **18b**. The guest inclusion in the complexes of **18** considerably increased the interlayer separations (6.913 Å in **18a** and 7.003 Å in **18b**) compared to that of **19** (5.224 Å). The benzonitrile and nitrobenzene molecules occupy the crystal volume of 30% in **18a** and **18b** respectively. Despite the similarities in the coordination connections of the layers in **18** and **19**, the ligands exhibit some geometrical differences. For example the interplanar angles between pyridine and central phenyl ring are 13.58° & 55.34° in **18a** and 13.48° & 53.91° in **18b**, while they are 76.59° and 81.03° in **19**. Therefore the metal-to-metal separation by the ligands is higher (10.459 Å) in **19** compared to those in **18** (10.001 Å in **18a**, 10.005 Å in **18b**).

Here it is interesting to note that, in case of **1e**, the use of other solvents such as nitrobenzene or toluene in place of $CHCl_3$ also resulted in single crystals of complex **19**, which indicates that the crystallization of complex **19** does not depend on the nature of the solvents. These reactions emphasize the fact that the host–host (aromatic) interactions are robust enough to allow crystallization of the complex. It is noteworthy that although the dimensionalities of the networks in **14**/**15**/**16** and **17**/**18**/**19** with respect to the coordination bonds differ, the layers are iso-structural in all the crystal structures with respect to amide-to-amide N–H···O hydrogen bonds.

Effect of guest molecules in templating CPs

It was mentioned earlier that the crystals of complexes **10** and **11** were obtained only by dissolving the crystals of complex **9** in DMF solution of excess biphenyl and pyrene respectively. This conversion found to be reversible that is by dissolving the crystals of **10** or **11** in the DMF solution of anthracene produces the crystals of **9**. The direct reactions to prepare complexes **10** and **11** failed to produce suitable crystals for single crystal X-ray analyses. However, the crystals of complex **9** can be prepared through the direct reaction by taking the ligand **2d**, $Cu(NO_3)_2$, NaSCN and anthracene in DMF–MeOH. These results indicate that the anthracene is acting as a better template than biphenyl or pyrene. To verify this fact, competitive reactions were performed by conducting the reactions in the presence of equal amounts of anthracene-pyrene or anthracene-biphenyl. In both the reactions, the crystals of **9** resulted selectively indicating that anthracene

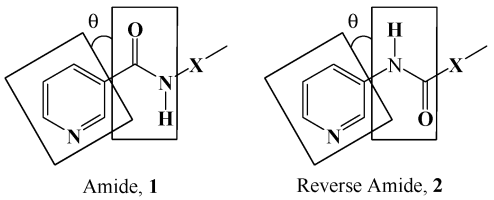

Scheme 3 Interplanar angle between the amide and pyridyl plane.

has a better template effect than the other two guest molecules. Similar reactions were also tried by dissolving complex **16**, which contains 9-anthraldehyde as guest, in the DMF solutions of anthracene, biphenyl or pyrene in anticipation of the crystals of **9**, **10** or **11** respectively. However these reactions does not resulted in the formation of these complexes. Also the preparation of the crystals of **16** by dissolving the complexes of **9**/**10**/**11** in DMF solution of 9-anthraldehyde was not successful.

Amide-to-amide hydrogen bonds

Our previous studies on crystal structures of analogues of **1** and **2** show that the amide-to-amide hydrogen bond occur only when the interplanar angle between pyridyl and amide plane is above 20° (Scheme 3). To see a similar correlation in coordination networks of these ligands, we have calculated these angles for all the structures reported here (Table 2). All the complexes which are not exhibiting amide to amide recognition have the interplanar angle values of less than 10° except in complex **13** (37.18°) where amide carbonyl is coordinating to the metal. On the other hand, not all the CPs containing amide-to-amide hydrogen bonds have the value of interplanar angle above 20°. In complexes **14–17** where the *β*-sheet recognition is present, it is observed that among the two angles one is close to 10° and the other is close to 50°. This discrepancy can be attributed to the arc like geometry of the ligand in these structures due to the geometry of the network. However, in complexes **18** and **19** where the ligand exhibits the linear geometry and also exhibit *β*-sheet contain the interplanar angles more than 20°. Similarly complex **7** which contain amide-to-amide recognition also exhibit interplanar angle of 25.30°. Therefore the values of interplanar angles obtained here are in accordance with our previous results.

Conclusion

Amides and reverse amides have shown the versatility in the formation of CPs with Cu(II) in the presence or the absence of guest molecules. The network geometries include 1D-chains and 2D networks with or without amide-to-amide recognition and with or without guest inclusion. The primary reason for the formation of 1D-chains may be due to the presence of other competing ligands such as counter anions, H_2O and solvent DMF in the reaction for the coordination to the metal centre. As the solvent DMF and counter anion thiocyanate has the coordination ability for metal; in most of the cases they inhibit the propagation of CPs to higher dimensions. Amide-to-amide recognition in the form of *β*-sheet was observed when the M:L ratios in the complexes are 1 : 2.

Nitrobenzene/benzonitrile inclusion favored in the complexes with the ligands containing shorter spacers –$(CH_2)_2$–, –$(CH_2)_4$– and phenyl over the ligands containing longer spacers –$(CH_2)_6$– & –$(CH_2)_8$– which preferred the inclusion of big size guest molecules such as anthracene, biphenyl, pyrene or phenanthrene. The reaction of ligand **2a** with Cu(II) resulted in three different CPs (**3**, **4** and **12**) revealing the different possible modes of aggregations by the same components. While the reactions with ligands **1a**, **1b** and **2c–e** with Cu(II) in the absence of guest molecules failed to produce crystalline complexes signifying the importance of guest molecules in these reactions. We note here that the complexes **10** and **11** can be synthesized only by dissolving the complex **9**, which are otherwise not possible to synthesize by direct reactions.

The ligands with phenyl, hexyl and octyl spacers have shown more consistency in exhibiting amide-to-amide hydrogen bonding recognition than the –$(CH_2)_2$– and –$(CH_2)_4$– spacers. The weak interactions between –$(CH_2)_6$– or –$(CH_2)_8$– or –C_6H_4– spacers tailor the consistent formation of the *β*-sheet. Similar observation was also made in the crystal structures of the ligands **1** and **2**. The iso-structurality between the coordination polymers of amides and reverse amides was observed with the ligands containing –$(CH_2)_6$– or phenyl spacers. Our efforts to grow the coordination polymers with mixed ligands using **1** and **2** in the same reaction were unsuccessful and always resulted in the complexes of **2**.

Experimental

General

FTIR spectra were recorded with a Perkin Elmer Instrument Spectrum Rx Serial No. 73713. Elemental analyses were obtained with a Perkin-Elmer instrument, series II, CHNS/O analyzer 2400. Thermogravimetric analysis (TGA) data were recorded with a Perkin-Elmer instrument, Pyris Diamond TG/DTA (air). The ligands were prepared according to procedures previously reported by us.[6]

Synthesis of complexes without aromatic guest

$\{Cu(2a)(SCN)_2(DMF)_2\}_n$ (3) and $\{[Cu(2a)(SCN)_2(DMF)_2]\cdot 2(DMF)\}_n$ (4). 54 mg (0.2 mmol) of **2a** dissolved in 3 mL DMF and to it was added a methanolic solution of $Cu(SCN)_2$, formed by addition of a MeOH (1 mL) solution of $Cu(NO_3)_2$ (24.16 mg, 0.1 mmol) to a MeOH (1 mL) solution of NaSCN (16.21 mg, 0.2 mmol). After a week green crystals were formed. Yield: ≈84%.

A similar procedure was adopted for the synthesis of complexes **5–8**.

$\{Cu(2b)(SCN)_2(DMF)_2\}_n$ (5). Yield: 87%; *Elemental analysis*: Calculated for $C_{24}H_{32}N_8O_4S_2Cu_1$: C, 46.18%; H, 5.13%; N, 17.96%; Found: C, 46.53%; H, 4.76%; N, 17.76%.

$\{[Cu(1c)(SCN)_2(H_2O)_2]\cdot 2(H_2O)\}_n$ (6). Yield: 54%; *Elemental analysis*: Calculated for $C_{20}H_{30}N_6O_6S_2Cu_1$ C, 41.55%; H, 5.23%; N, 14.54%; Found: C, 41.76%; H, 5.13%; N, 14.72%.

{[Cu(1d)(SCN)$_2$(DMF)$_2$]·2(H$_2$O)}$_n$ (7). Yield: 22%; *Elemental analysis*: Calculated for $C_{28}H_{44}N_8O_6S_2Cu_1$: C, 46.94%; H, 6.19%; N, 15.64%; Found: C, 46.57%; H, 6.05%; N, 15.93%.

{[Cu(1e)(SCN)$_2$(DMF)$_2$]·2(DMF)}$_n$ (8). Yield: 54%; *Elemental analysis*: Calculated for $C_{32}H_{42}N_{10}O_6S_2Cu_1$: C, 48.63%; H, 5.36%; N, 17.72%; Found: C, 48.81%; H, 5.19%; N, 17.23%.

{Cu(1e)$_2$(SCN)$_2$}$_n$ (19). A methanolic solution of $Cu(SCN)_2$, formed by addition of a MeOH (0.5 mL) solution of $Cu(NO_3)_2$ (15.2 mg, 0.063 mmol) to a MeOH (0.5 mL) solution of NaSCN (10.2 mg, 0.126 mmol), was carefully layered onto an ethanol (1 mL)/$CHCl_3$ (5.0 mL) solution (6.0 mL) of **1e** (40.0 mg, 0.126 mmol). Light green crystals were formed after a week. Yield: 20%; *Elemental analysis*: Calculated for $C_{38}H_{28}N_{10}O_4S_2Cu_1$: C 55.9%, H 3.4%, N 17.1%; Found: C 55.0%, H 2.9%, N 16.8%.

Synthesis of complexes with aromatic guest

{[Cu(2d)(SCN)$_2$(DMF)$_2$] (anthracene)}$_n$ (9). 70.8 mg (0.2 mmol) of **1a** and 178 mg of anthracene (1.0 mmol) (for liquid guest 2 ml) dissolved in 3 mL DMF and to it was added a methanolic solution of $Cu(SCN)_2$. After a week green crystals were formed. Yield: 79%; *Elemental analysis*: Calculated for $C_{42}H_{50}N_8O_4S_2Cu_1$: C, 58.77%; H, 5.83%; N, 13.06%; Found: C, 59.04%; H, 5.57%; N, 13.08%.

Good quality crystals of **10** and **11** were obtained by dissolving complex **13** with biphenyl or pyrene guest molecules.

{[Cu(2d)(SCN)$_2$(DMF)$_2$]·(biphenyl)}$_n$ (10). Yield: 76%; *Elemental analysis*: Calculated for $C_{40}H_{52}N_8O_4S_2Cu_1$: C, 57.44%; H, 6.22%; N, 13.40%; Found: C, 57.83%; H, 5.99%; N, 13.62%.

{[Cu(2d)(SCN)$_2$(DMF)$_2$]·(pyrene)}$_n$ (11). Yield: 68%; *Elemental analysis*: Calculated for $C_{44}H_{52}N_8O_4S_2Cu_1$: C, 59.74%; H, 5.92%; N, 12.67%; Found: C, 60.17%; H, 5.70%; N, 12.33%.

{[Cu(2a)(SCN)$_2$]·2(DMF)·(nitrobenzene)}$_n$ (12). Yield: ≈76%.

{[Cu(1b)(SCN)$_2$]·2(nitrobenzene)}$_n$ (13). Yield: 68%; *Elemental analysis*: Calculated for $C_{30}H_{28}N_8O_6S_2Cu_1$: C, 49.75%; H, 3.90%; N, 15.47%; Found: C, 49.58%; H, 3.71%; N, 15.34%.

{[Cu(1c)$_2$(SCN)$_2$]·2(di-bromobenzene)}$_n$ (14a). Yield: 46%; *Elemental analysis*: Calculated for $C_{50}H_{52}N_{10}O_4S_2Br_4Cu_1$: C, 48.40%; H, 4.19%; N, 11.29%; Found: C, 48.07%; H, 4.62%; N, 10.94%.

{[Cu(1c)$_2$(SCN)$_2$]·2(phenanthrene)}$_n$ (14b). Yield: 44%; *Elemental analysis*: Calculated for $C_{66}H_{64}N_{10}O_4S_2Cu_1$: C, 66.69%; H, 5.38%; N, 11.79%; Found: C, 66.68%; H, 5.31%; N, 12.08%.

{[Cu(2c)$_2$(SCN)$_2$]·2(di-iodobenzene)}$_n$ (15a). Yield: 62%; *Elemental analysis*: Calculated for $C_{50}H_{52}N_{10}O_4S_2I_4Cu_1$: C, 40.22%; H, 3.49%; N, 9.39%; Found: C, 40.85%; H, 3.64%; N, 9.74%.

{[Cu(2c)$_2$(SCN)$_2$]·2(phenanthrene)}$_n$ (15b). Yield: 65%; *Elemental analysis*: Calculated for $C_{66}H_{64}N_{10}O_4S_2Cu_1$: C, 66.69%; H, 5.38%; N, 11.79%; Found: C, 67.30%; H, 5.33%; N, 11.95%.

{[Cu(2c)$_2$(SCN)$_2$]·2(di-bromobenzene)}$_n$ (15c). Yield: 52%; *Elemental analysis*: Calculated for $C_{50}H_{52}N_{10}O_4S_2Br_4Cu_1$: C, 48.40%; H, 4.19%; N 11.29,%; Found: C, 47.95%; H, 3.78%; N, 10.69%.

{[Cu(2c)$_2$(SCN)$_2$]·2(pyrene)}$_n$ (15d). Yield: 43%; *Elemental analysis*: Calculated for $C_{70}H_{68}N_{10}O_4S_2Cu_1$: C, 67.98%; H, 5.18%; N, 11.33%; Found: C, 68.13%; H, 5.24%; N, 11.62%.

{[Cu(2d)$_2$(SCN)$_2$]·2(9-anthraldehyde)}$_n$ (16). Yield: 72%; *Elemental analysis*: Calculated for $C_{72}H_{72}N_{10}O_6S_2Cu_1$: C, 66.47%; H, 5.58%; N, 10.77%; Found: C, 66.38%; H, 5.34%; N, 10.88%.

{[Cu(1a)$_2$(SCN)$_2$]·6(nitrobenzene)}$_n$ (17). Yield: 66%; *Elemental analysis*: Calculated for $C_{66}H_{58}N_{16}O_{16}S_2Cu_1$: C, 54.33%; H, 3.97%; N, 15.35%; Found: C 53.48%, H 3.71%, N 15.02%.

{(Cu(2e)$_2$(SCN)$_2$)·2(benzonitrile)}$_n$ (18a). Layering technique is applied in which metal in methanol layered over the mixture of DMF-Benzonitrile solution. Yield: 33%; *Elemental analysis*: Calculated for $C_{66}H_{64}N_{10}O_4S_2Cu_1$: C, 61.08%; H, 3.72%; N, 16.44%; Found: C, 60.42%; H, 3.53%; N, 16.31%.

{(Cu(2e)$_2$(SCN)$_2$)·2(nitrobenzene)}$_n$ (18b). A similar procedure to **18a** was adopted for the synthesis this complex. Yield: 26%; *Elemental analysis*: Calculated for $C_{50}H_{38}N_{12}O_8S_2Cu_1$: C, 56.52%; H, 3.60%; N, 15.82%; Found: C, 56.23%; H, 3.47%; N, 15.44%.

X-Ray crystallography

The single crystal data was collected on Bruker APEX-2 CCD X-ray diffractometer that uses graphite monochromated Mo-Kα radiation (λ = 0.71073 Å) by hemisphere method. The structures are solved by direct methods and refined by least square methods on F^2 using SHELX-97.[10] Non-hydrogen atoms were refined anisotropically and hydrogen atoms were fixed at calculated positions and refined using a riding model. PLATON is used for the calculation of guest available volumes.[11] DMF molecules in the complexes **3**, **8** and **10** exhibited disorder, which have been modeled and refined. In **7**, the disorder in NMe_2 group of DMF and water molecules could not be modeled. Therefore, the final structure of **7** was refined using squeeze option without NMe_2 group of DMF and H_2O molecules.

Acknowledgements

We gratefully acknowledge financial support from DST, DST-FIST for single crystal X-ray facility. LR thanks IIT (Kharagpur) for research fellowship.

References

1 (*a*) A. F. Wells, *Three dimensional Nets and Polyhedra*, Wiley-Interscience, New York, 1977; (*b*) S. R. Batten and R. Robson, *Angew. Chem., Int. Ed.*, 1998, **37**, 1460;

(*c*) P. J. Hagrman, D. Hagrman and J. Zubieta, *Angew. Chem., Int. Ed.*, 1999, **38**, 2638; (*d*) B. Moulton and M. J. Zaworotko, *Chem. Rev.*, 2001, **101**, 1629; (*e*) R. J. Hill, D.-L. Long, N. R. Champness, P. Hubberstey and M. Schröder, *Acc. Chem. Res.*, 2005, **38**, 335; (*f*) D. J. Tranchemontagne, Z. Ni, M. O'Keeffe and O. M. Yaghi, *Angew. Chem., Int. Ed.*, 2008, **47**, 5136.

2 (*a*) O. M. Yaghi, H. Li, C. Davis, D. Richardson and T. L. Groy, *Acc. Chem. Res.*, 1998, **31**, 474; (*b*) K. Biradha and M. Fujita, *Angew. Chem., Int. Ed.*, 2002, **41**, 3392; (*c*) C. Janiak, *Dalton Trans.*, 2003, 2781; (*d*) S. L. James, *Chem. Soc. Rev.*, 2003, **32**, 276; (*e*) K. Biradha, *CrystEngComm*, 2003, **5**, 374; (*f*) S. Kitagawa, R. Kitaura and S. Noro, *Angew. Chem., Int. Ed.*, 2004, **43**, 2334; (*g*) S. R. Batten, *J. Solid State Chem.*, 2005, **178**, 2475; (*h*) N. C. Gianneschi, M. S. Masar and C. A. Mirkin, *Acc. Chem. Res.*, 2005, **38**, 825; (*i*) G. J. Halder and C. J. Kepert, *J. Am. Chem. Soc.*, 2005, **127**, 7891; (*j*) P. L. Llewellyn, S. Bourrelly, C. Serre, Y. Filinchuk and G. Férey, *Angew. Chem., Int. Ed.*, 2006, **45**, 7751; (*k*) M. H. Filby and J. W. Steed, *Coord. Chem. Rev.*, 2006, **250**, 3200; (*l*) M. Kawano and M. Fujita, *Coord. Chem. Rev.*, 2007, **251**, 2592; (*m*) R. Banerjee, A. Phan, B. Wang, C. Knobler, H. Furukawa, M. O'Keeffe and O. M. Yaghi, *Science*, 2008, **319**, 939; (*n*) D. Farrusseng, S. Aguado and C. Pinel, *Angew. Chem., Int. Ed.*, 2009, **48**, 7502; (*o*) T. Uemura, N. Yanai and S. Kitagawa, *Chem. Soc. Rev.*, 2009, **38**, 1228; (*p*) K. Li, D. H. Olson, J. Seidel, T. J. Emge, H. Gong, H. Zeng and J. Li, *J. Am. Chem. Soc.*, 2009, **131**, 10368; (*q*) K. M. L. Taylor-Pashow, J. D. Rocca, Z. Xie, S. Tran and W. Lin, *J. Am. Chem. Soc.*, 2009, **131**, 14261; (*r*) K. A. Cychosz, A. G. Wong-Foy and A. J. Matzger, *J. Am. Chem. Soc.*, 2009, **131**, 14538; (*s*) J.-R. Li, R. J. Kuppler and H.-C. Zhou, *Chem. Soc. Rev.*, 2009, **38**, 1477.

3 (*a*) M. Fujita, K. Umemoto, M. Yoshizawa, N. Fujita, T. Kusukawa and K. Biradha, *Chem. Commun.*, 2001, 509; (*b*) D. T. Vodak, M. E. Braun, J. Kim, M. Eddaoudi and O. M. Yaghi, *Chem. Commun.*, 2001, 2534; (*c*) K. Biradha and M. Fujita, *Angew. Chem., Int. Ed.*, 2002, **41**, 3392; (*d*) N. G. Pschirer, D. M. Ciurtin, M. D. Smith, H. F. Bunz and H.-C. zur Loye, *Angew. Chem., Int. Ed.*, 2002, **41**, 583; (*e*) A. C. Sudik, N. W. Ockwig, A. R. Millward, A. P. Côté and O. M. Yaghi, *J. Am. Chem. Soc.*, 2005, **127**, 7110; (*f*) L. Carlucci, G. Ciani, D. M. Proserpio and F. Porta, *CrystEngComm*, 2005, **7**, 78; (*g*) K. Biradha, M. Sarkar and L. Rajput, *Chem. Commun.*, 2006, 4169; (*h*) Y. Zou, S. Hong, M. Park, H. Chun and M. S. Lah, *Chem. Commun.*, 2007, 5182; (*i*) G. Mahmoudi and A. Morsali, *CrystEngComm*, 2007, **9**, 1062; (*j*) C.-D. Wu, L. Ma and W. Lin, *Inorg. Chem.*, 2008, **47**, 11446; (*k*) L. Hou, Y.-Y. Lin and X.-M. Chen, *Inorg. Chem.*, 2008, **47**, 1346; (*l*) M. H. Alkordi, Y. Liu, R. W. Larsen, J. F. Eubank and M. Eddaoudi, *J. Am. Chem. Soc.*, 2008, **130**, 12639; (*m*) Z.-B. Han, J.-W. Ji, H.-Y. An, W. Zhang, G.-X. Han, G.-X. Zhanga and L.-G. Yang, *Dalton Trans.*, 2009, 9807; (*n*) Q. Yue, Q. Sun, A.-L. Cheng and E.-Q. Gao, *Cryst. Growth Des.*, 2010, **10**, 44.

4 (*a*) M. Fujita and K. Ogura, *Bull. Chem. Soc. Jpn.*, 1996, **73**, 1369; (*b*) S. Muthu, J. H. K. Yip and J. J. Vittal, *J. Chem. Soc., Dalton Trans.*, 2001, 3577; (*c*) V. Balamurugan and R. Mukherjee, *CrystEngComm*, 2005, **7**, 337; (*d*) X.-Q. Lu, M. Pan, J.-R. He, Y.-P. Cai, B.-S. Kanga and C.-Y. Su, *CrystEngComm*, 2006, **8**, 827; (*e*) G. L. Spina, R. Clérac, E. S. Collins, T. McCabe, M. Venkatesan, I. Ichinose and W. Schmitt, *Dalton Trans.*, 2007, 5248; (*f*) J. J. Perry, V. Ch. Kravtsov, G. J. McManus and M. J. Zaworotko, *J. Am. Chem. Soc.*, 2007, **129**, 10076; (*g*) Q. Zhang, X. Bu, Z. Lin, T. Wu and P. Feng, *Inorg. Chem.*, 2008, **47**, 9724; (*h*) L. Rajput and K. Biradha, *Cryst. Growth Des.*, 2007, **7**, 2376; (*i*) S. K. Chandran, R. Thakuria and A. Nangia, *CrystEngComm*, 2008, **10**, 1891; (*j*) P. K. Thallapally, J. Tian, M. Radha Kishan, C. A. Fernandez, S. J. Dalgarno, P. B. McGrail, J. E. Warren and J. L. Atwood, *J. Am. Chem. Soc.*, 2008, **130**, 16842; (*k*) X.-D. Chen, X.-H. Zhao, M. Chen and M. Du, *Chem.–Eur. J.*, 2009, **15**, 12974; (*l*) C. Xie, L. Zhou, W. Feng, J. Wang and W. Chen, *J. Mol. Struct.*, 2009, **921**, 132; (*m*) J.-Q. Chen, Y.-P. Cai, H.-C. Fang, Z.-Y. Zhou, X.-L. Zhan, G. Zhao and Z. Zhang, *Cryst. Growth Des.*, 2009, **9**, 1605; (*n*) P. Lama, A. Aijaz, E. C. Sañudo and P. K. Bharadwaj, *Cryst. Growth Des.*, 2010, **10**, 283.

5 (*a*) P. L. Jones, K. J. Byrom, J. C. Jeffery, J. A. McCleverty and M. D. Ward, *Chem. Commun.*, 1997, 1361; (*b*) T. C. Hennigar, D. C. MacQuarrie, P. Losier, R. D. Rogers and M. J. Zaworotko, *Angew. Chem., Int. Ed. Engl.*, 1997, **36**, 972; (*c*) D. L. Caulder, R. E. Powers, T. N. Parac and K. N. Raymond, *Angew. Chem., Int. Ed.*, 1998, **37**, 1840; (*d*) J. S. Fleming, K. L. V. Mann, C.-A. Carraz, E. Psillakis, J. C. Jeffery, J. A. McCleverty and M. D. Ward, *Angew. Chem., Int. Ed.*, 1998, **37**, 1279; (*e*) R. Vilar, D. M. P. Mingos, A. J. P. White and D. J. Williams, *Angew. Chem., Int. Ed.*, 1998, **37**, 1258; (*f*) S. Lopez and S. W. Keller, *Inorg. Chem.*, 1999, **38**, 1883; (*g*) M. A. Withersby, A. J. Blake, N. R. Champness, P. A. Cooke, P. Hubberstey, W.-S. Li and M. Schröder, *Inorg. Chem.*, 1999, **38**, 2259; (*h*) C. He, B.-G. Zhang, C.-Y. Duan, J.-H. Li and Q.-J. Meng, *Eur. J. Inorg. Chem.*, 2000, 2549; (*i*) R. L. Paul, S. M. Couchman, J. C. Jeffery, J. A. McCleverty, Z. R. Reeves and M. D. Ward, *J. Chem. Soc., Dalton Trans.*, 2000, 845; (*j*) K. S. Min and M. P. Suh, *J. Am. Chem. Soc.*, 2000, **122**, 6834; (*k*) L. Pan, T. Frydel, M. B. Sander, X. Huang and J. Li, *Inorg. Chem.*, 2001, **40**, 1271; (*l*) Y. Kang, S. S. Lee, K.-M. Park, S. H. Lee, S. O. Kang and J. Ko, *Inorg. Chem.*, 2001, **40**, 7027; (*m*) M. J. Hannon, C. L. Painting, E. A. Plummer, L. J. Childs and N. W. Alcock, *Chem.–Eur. J.*, 2002, **8**, 2225; (*n*) M. Dua, S.-T. Chena, X.-H. Bua and J. Ribas, *Inorg. Chem. Commun.*, 2002, **5**, 1003; (*o*) S. Noro, R. Kitaura, M. Kondo, S. Kitagawa, T. Ishii, H. Matsuzaka and M. Yamashita, *J. Am. Chem. Soc.*, 2002, **124**, 2568; (*p*) P. D. Beer and E. J. Hayes, *Coord. Chem. Rev.*, 2003, **240**, 167; (*q*) S. J. Dalgarno, M. J. Hardie and C. L. Raston, *Cryst. Growth Des.*, 2004, **4**, 227; (*r*) J.-R. Li, X. H. Bu and R.-H. Zhang, *Dalton Trans.*, 2004, 813; (*s*) J. M. Russel, A. D. M. Parker, I. R. Evans, J. A. K. Howard and J. W. Steed, *CrystEngComm*, 2006, **8**, 119; (*t*) P. Diaz, J. Benet-Buchholz, R. Vilar and A. J. P. White, *Inorg. Chem.*, 2006, **45**, 1617; (*u*) Q. Yu, X. Zhang, H. Bian, H. Liang, B. Zhao, S. Yan and D. Liao, *Cryst. Growth Des.*, 2008, **8**, 1140; (*v*) G.-C. Xu, Q. Hua, T. Okamura, Z.-S. Bai, Y.-J. Ding, Y.-Q. Huang, G.-X. Liu, W.-Y. Sun and N. Ueyama, *CrystEngComm*, 2009, **11**, 261.

6 (*a*) M. Sarkar and K. Biradha, *Cryst. Growth Des.*, 2006, **6**, 202; (*b*) L. Rajput, S. Singha and K. Biradha, *Cryst. Growth Des.*, 2007, **7**, 2788.

7 (*a*) M. Sarkar and K. Biradha, *Cryst. Growth Des.*, 2007, **7**, 1318; (*b*) M. Sarkar and K. Biradha, *Cryst. Growth Des.*, 2006, **6**, 1742; (*c*) M. Sarkar and K. Biradha, *Chem. Commun.*, 2005, 2229; (*d*) M. Sarkar and K. Biradha, *Eur. J. Inorg. Chem.*, 2006, 531; (*e*) L. Rajput and K. Biradha, *Polyhedron*, 2008, **27**, 1248; (*f*) L. Rajput and K. Biradha, *Cryst. Growth Des.*, 2009, **9**, 3848; (*g*) L. Rajput and K. Biradha, *CrystEngComm*, 2009, **11**, 1220.

8 (*a*) D. R. Turner, B. Smith, E. C. Spencer, A. E. Goeta, I. R. Evans, D. A. Tocher, J. A. K. Howard and J. W. Steed, *New J. Chem.*, 2005, **29**, 90; (*b*) D. Krishna Kumar, A. Das and P. Dastidar, *CrystEngComm*, 2006, **8**, 805; (*c*) R. Custelcean, B. A. Moyer, V. S. Bryantsev and B. P. Hay, *Cryst. Growth Des.*, 2006, **6**, 555; (*d*) D. Krishna Kumar, A. Das and P. Dastidar, *Cryst. Growth Des.*, 2007, **7**, 2096.

9 (*a*) K. Uemura, S. Kitagawa, K. Fukui and K. Saito, *J. Am. Chem. Soc.*, 2004, **126**, 3817; (*b*) K. Uemura, K. Saito, S. Kitagawa and H. Kita, *J. Am. Chem. Soc.*, 2006, **128**, 16122; (*c*) K. Uemura, S. Kitagawa, M. Kondo, K. Fukui, R. Kitaura, H.-C. Chang and T. Mizutani, *Chem.–Eur. J.*, 2002, **8**, 3586; (*d*) K. Uemura, Y. Kumamoto and S. Kitagawa, *Chem.–Eur. J.*, 2008, **14**, 9565.

10 G. M. Sheldrick, *SHELX-97, Program for the Solution and Refinement of Crystal Structures*, University of Göttingen, Göttingen, Germany, 1997.

11 A. L. Spek, *PLATON, A Multi Purpose Crystallographic Tool*, Utrecht University, Utrecht, The Netherlands, 2002.

